文章编号:1000-0887(2004)01-0022-13

热-压电效应对轴压混合层合圆柱曲板后屈曲的影响*

沈惠申

(上海交通大学 建筑工程与力学学院,上海 200030)

(我刊编委沈惠申来稿)

摘要: 基于 Kármán-Donnell 型非线性壳体方程,给出带压电作动器混合层合圆柱曲板在机械荷载、电荷载和热荷载作用下的后屈曲分析. 假定温度场为均匀分布,电场仅有沿板厚方向的分量 E_Z,且假定材料性能常数与温度和电场的变化无关. 将壳体屈曲的边界层理论推广到混合层合圆柱曲板受复合荷载作用的情况. 相应的奇异摄动法用于确定圆柱曲板的屈曲荷载和后屈曲平衡路径. 分析中同时考虑非线性前屈曲变形和初始几何缺陷的影响. 数值算例给出完善和非完善,含整体覆盖或内埋压电作动器正交铺设层合圆柱曲板的后屈曲平衡路径. 讨论了温度变化、控制电压、铺层方式、面内边界条件和初始几何缺陷等各种参数变化的影响.

关 键 词: 后屈曲; 混合层合圆柱曲板; 热-压电效应; 壳体屈曲的边界层理论; 奇异摄动法

中图分类号: O343 **文献标识码:** A

引 言

复合材料层合圆柱曲板已广泛用作航空构件. 含智能材料的智能结构的出现代表着材料和结构工程的最新进展. 含压电层复合材料混合结构可以综合压电材料和纤维增强复合材料层合结构的双重优点. 因而,含表面整体覆盖或内埋压电传感器和(或)作动器的混合层合结构的研究变得越来越重要.

文献[1~3]给出过混合层合圆柱曲板的建模和分析,主要集中在线性弯曲和振动控制方面. 最近,Oh 等[4]给出上下表面贴有压电作动器的层合板的热后屈曲分析. 分析中采用基于"分层理论"的有限元算式,但其数值结果仅限于无初始几何缺陷的完善薄板. Shen[5,6]分别给出含表面整体覆盖或内埋压电作动器的圆柱薄壳在复合荷载作用下的完整的后屈曲和热后屈曲分析. 分析中同时考虑非线性前屈曲变形和初始几何缺陷的影响. 然而,至今尚无公开发表的文献讨论过混合层合圆柱曲板在轴压和热环境中的后屈曲行为.

本文基于 Kármán-Donnell 型非线性壳体方程,将 Shen 和 Chen[7,8]提出的壳体屈曲的边界

* **收稿日期:** 2002-05-14; **修订日期:** 2003-07-26
基金项目: 国家自然科学基金资助项目(50375091)
作者简介: 沈惠申(1947—),男,浙江嘉善人,教授,博士,博士生导师(Tel:86-21-64956627; E-mail: hsshen@mail.sjtu.edu.cn).

层理论推广到混合层合圆柱曲板受复合荷载作用的情况．假定温度场为均匀分布，电场仅有沿板厚方向的分量 E_Z．事实上温度的变化将影响到纤维增强复合材料的材料性能常数[9]．另一方面，压电材料的性能常数，如压电应变常数等，都会因温度的变化而变化[10]．本文中暂不考虑这些因素，即假定材料性能常数与温度和电场的变化无关．奇异摄动法用于确定圆柱曲板的屈曲荷载和后屈曲平衡路径．分析中同时考虑非线性前屈曲变形和初始几何缺陷的影响，初始几何缺陷的形式取作和曲板初始屈曲模态一致．

1　基本理论和控制方程

考虑由压电材料和纤维增强复合材料构成的混合层合圆柱曲板．假定 $\bar{U}$、$\bar{V}$ 和 $\bar{W}$ 为对应右手坐标系 (X, Y, Z) 的位移分量，其中 X，Y 和 Z 分别为曲板中面轴向，周向和法向（向内指向为正）坐标．坐标原点取在曲板中面角点．R 为曲率半径，t 为曲板厚度，a 为曲板长度，b 为曲板弧线宽度，如图 1 所示．假定圆柱曲板相对较薄且几何非完善，受到轴向压缩及热荷载和电荷载的共同作用．以 $\bar{W}^*(X, Y)$ 和 $\bar{W}(X, Y)$ 分别表示曲板的初始几何缺陷和附加的挠度，以 $\bar{F}(X, Y)$ 表示应力函数，即使 $\bar{N}_x = \bar{F}_{,yy}$，$\bar{N}_y = \bar{F}_{,xx}$ 和 $\bar{N}_{xy} = -\bar{F}_{,xy}$，其中逗号表示对相应坐标求导．

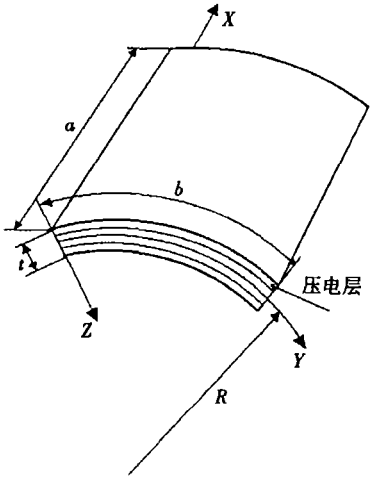

图 1　含压电层合圆柱曲板几何尺寸和坐标系

基于经典 Donnell 壳体理论（即不考虑横向剪切变形的影响），采用 Kármán 位移-应变关系，并计及热-压电效应，我们可以导得以法向挠度 $\bar{W}$（含初始几何缺陷 $\bar{W}^*$）和应力函数 $\bar{F}$ 表示的广义 Kármán-Donnell 型非线性壳体方程

$$\tilde{L}_{11}(\bar{W}) + \tilde{L}_{12}(\bar{F}) - \tilde{L}_{13}(\bar{N}^P) - \tilde{L}_{14}(\bar{M}^P) - \frac{1}{R}\bar{F}_{,xx} = \tilde{L}(\bar{W} + \bar{W}^*, \bar{F}), \tag{1}$$

$$\tilde{L}_{21}(\bar{F}) - \tilde{L}_{22}(\bar{W}) - \tilde{L}_{23}(\bar{N}^P) + \frac{1}{R}\bar{W}_{,xx} = -\frac{1}{2}\tilde{L}(\bar{W} + 2\bar{W}^*, \bar{F}), \tag{2}$$

其中线性算子 $\tilde{L}_{ij}(\ )$ 和非线性算子 $\tilde{L}(\ )$ 如文献[5]所给出．

上式中等效热-压电力和弯矩定义为

$$\begin{bmatrix} \bar{N}^P \\ \bar{M}^P \end{bmatrix} = \begin{bmatrix} \bar{N}^T \\ \bar{M}^T \end{bmatrix} + \begin{bmatrix} \bar{N}^E \\ \bar{M}^E \end{bmatrix}. \tag{3}$$

假定温度场是均匀热场，电场仅有沿板厚方向的分量 E_Z，即

$$E_Z = \frac{V_k}{t_k}, \tag{4}$$

其中 V_k 为第 k 层层板的控制电压，t_k 是第 k 层层板的厚度．那么，温度改变 ΔT 和电场引起的力和弯矩定义为

$$\begin{bmatrix} \bar{N}_x^T & \bar{M}_x^T \\ \bar{N}_y^T & \bar{M}_y^T \\ \bar{N}_{xy}^T & \bar{M}_{xy}^T \end{bmatrix} = \sum_{k=1}^{N} \int_{t_{k-1}}^{t_k} \begin{bmatrix} A_x \\ A_y \\ A_{xy} \end{bmatrix}_k \Delta T(1, Z)\mathrm{d}Z \tag{5a}$$

及

$$\begin{bmatrix} \bar{N}_x^E & \bar{M}_x^E \\ \bar{N}_y^E & \bar{M}_y^E \\ \bar{N}_{xy}^E & \bar{M}_{xy}^E \end{bmatrix} = \sum_{k=1}^{N} \int_{t_{k-1}}^{t_k} \begin{bmatrix} B_x \\ B_y \\ B_{xy} \end{bmatrix}_k \frac{V_k}{t_k}(1, Z)\mathrm{d}Z, \tag{5b}$$

其中

$$\begin{bmatrix} A_x \\ A_y \\ A_{xy} \end{bmatrix} = -\begin{bmatrix} \bar{Q}_{11} & \bar{Q}_{12} & \bar{Q}_{16} \\ \bar{Q}_{12} & \bar{Q}_{22} & \bar{Q}_{26} \\ \bar{Q}_{16} & \bar{Q}_{26} & \bar{Q}_{66} \end{bmatrix} \begin{bmatrix} c^2 & s^2 \\ s^2 & c^2 \\ 2cs & -2cs \end{bmatrix} \begin{bmatrix} \alpha_{11} \\ \alpha_{22} \end{bmatrix}, \tag{6a}$$

$$\begin{bmatrix} B_x \\ B_y \\ B_{xy} \end{bmatrix} = -\begin{bmatrix} \bar{Q}_{11} & \bar{Q}_{12} & \bar{Q}_{16} \\ \bar{Q}_{12} & \bar{Q}_{22} & \bar{Q}_{26} \\ \bar{Q}_{16} & \bar{Q}_{26} & \bar{Q}_{66} \end{bmatrix} \begin{bmatrix} c^2 & s^2 \\ s^2 & c^2 \\ 2cs & -2cs \end{bmatrix} \begin{bmatrix} d_{31} \\ d_{32} \end{bmatrix}, \tag{6b}$$

其中 α_{11} 和 α_{22} 为第 k 层层板纵向和横向热膨胀系数，d_{31} 和 d_{32} 为第 k 层层板的压电应变常数．$\bar{Q}_{ij}$ 为转换弹性常数，由常规方法给出(见 Shen[5])．

边界支承假定为四边简支的，且考虑两种面内边界条件，即非加载直线边界面内可移和面内不可移．那么，边界条件为

$X = 0, a$:

$$\bar{W} = \bar{V} = 0, \tag{7a}$$

$$\bar{M}_x = -B_{21}^* \frac{\partial^2 \bar{F}}{\partial X^2} - B_{11}^* \frac{\partial^2 \bar{F}}{\partial Y^2} + B_{61}^* \frac{\partial^2 \bar{F}}{\partial X \partial Y} - D_{11}^* \frac{\partial^2 \bar{W}}{\partial X^2} - D_{12}^* \frac{\partial^2 \bar{W}}{\partial Y^2} - 2D_{16}^* \frac{\partial^2 \bar{W}}{\partial X \partial Y} + \bar{M}_x^P = 0, \tag{7b}$$

$$\int_0^b \bar{N}_x \mathrm{d}Y + \sigma_x tb = 0. \tag{7c}$$

$Y = 0, b$:

$$\bar{W} = 0, \tag{7d}$$

$$\bar{N}_{xy} = 0, \tag{7e}$$

$$\bar{M}_y = -B_{12}^* \frac{\partial^2 \bar{F}}{\partial Y^2} - B_{22}^* \frac{\partial^2 F}{\partial X^2} + B_{62}^* \frac{\partial^2 \bar{F}}{\partial X \partial Y} - D_{12}^* \frac{\partial^2 \bar{W}}{\partial X^2} - D_{22}^* \frac{\partial^2 \bar{W}}{\partial Y^2} - 2D_{26}^* \frac{\partial^2 \bar{W}}{\partial X \partial Y} + \bar{M}_y^P = 0$$

或

$$\bar{W}_{,x} = 0, \tag{7f}$$

$$\int_0^a \bar{N}_y \mathrm{d}X = 0 \text{（面内可移）或 } \bar{V} = 0 \text{（面内不可移）}, \tag{7g}$$

其中 σ_x 为平均压应力，$\bar{M}_x$ 和 $\bar{M}_y$ 为单位长度弯矩．对于对称铺设层合圆柱曲板式(7f)取 $\bar{M}_y = 0$，对于非对称铺设层合圆柱曲板由于存在拉-弯耦合效应 $\bar{M}_y = 0$ 的条件无法精确满足，因而用 $\bar{W}_{,x} = 0$ 取代 $\bar{M}_y = 0$ 的条件．面内不可移条件 $\bar{V} = 0$(沿 $Y = 0, b$ 边界)可用其均值代替，即

$$\int_0^a \int_0^b \frac{\partial \bar{V}}{\partial Y} \mathrm{d}Y \mathrm{d}X = 0, \tag{8a}$$

或

$$\int_0^a \int_0^b \left[\left(A_{22}^* \frac{\partial^2 \bar{F}}{\partial X^2} + A_{12}^* \frac{\partial^2 \bar{F}}{\partial Y^2} \right) - \left(B_{21}^* \frac{\partial^2 \bar{W}}{\partial X^2} + B_{22}^* \frac{\partial^2 \bar{W}}{\partial Y^2} \right) + \right.$$

$$\frac{\bar{W}}{R} - \frac{1}{2}\left(\frac{\partial \bar{W}}{\partial Y}\right)^2 - \frac{\partial \bar{W}}{\partial Y}\frac{\partial \bar{W}^*}{\partial Y} - (A_{12}^* \bar{N}_x^p + A_{22}^* \bar{N}_y^p)\Big]\mathrm{d}Y\mathrm{d}X = 0. \tag{8b}$$

曲板的平均端部缩短,含有热-压电引起的面力,可表为

$$\frac{\Delta x}{a} = -\frac{1}{ab}\int_0^b\int_0^a \frac{\partial \bar{U}}{\partial X}\mathrm{d}X\mathrm{d}Y =$$
$$-\frac{1}{ab}\int_0^b\int_0^a\Big[\left(A_{11}^* \frac{\partial^2 \bar{F}}{\partial Y^2} + A_{12}^* \frac{\partial^2 \bar{F}}{\partial X^2}\right) - \left(B_{11}^* \frac{\partial^2 \bar{W}}{\partial X^2} + B_{12}^* \frac{\partial^2 \bar{W}}{\partial Y^2}\right) -$$
$$\frac{1}{2}\left(\frac{\partial \bar{W}}{\partial X}\right)^2 - \frac{\partial \bar{W}}{\partial X}\frac{\partial \bar{W}^*}{\partial X} - (A_{11}^* \bar{N}_x^p + A_{12}^* \bar{N}_y^p)\Big]\mathrm{d}X\mathrm{d}Y. \tag{9}$$

上式中 $[A_{ij}^*]$, $[B_{ij}^*]$ 和 $[D_{ij}^*]$ $(i, j = 1, 2, 6)$ 为"约化"刚度矩阵, 定义为 $\boldsymbol{A}^* = \boldsymbol{A}^{-1}$, $\boldsymbol{B}^* = -\boldsymbol{A}^{-1}\boldsymbol{B}$, $\boldsymbol{D}^* = \boldsymbol{D} - \boldsymbol{B}\boldsymbol{A}^{-1}\boldsymbol{B}$,其中 $\boldsymbol{A}$, $\boldsymbol{B}$ 和 $\boldsymbol{D}$ 由常规方法给出.

2　分析方法与渐近解

这一节我们结合边界条件(7)来求解方程(1)和(2). 令

$$\begin{bmatrix} A_x^T \\ A_y^T \end{bmatrix}\Delta T = -\sum_{k=1}^{N}\int_{t_{k-1}}^{t_k}\begin{bmatrix} A_x \\ A_y \end{bmatrix}_k \Delta T\mathrm{d}Z, \tag{10a}$$

$$\begin{bmatrix} B_x^p \\ B_y^p \end{bmatrix}\Delta V = -\sum_{k=1}^{N}\int_{t_{k-1}}^{t_k}\begin{bmatrix} B_x \\ B_y \end{bmatrix}_k \frac{V_k}{t_k}\mathrm{d}Z. \tag{10b}$$

并引进无量纲参数

$$\begin{cases} x = \pi X/a,\ y = \pi Y/b,\ \beta = a/b, \\ \bar{Z} = a^2/Rt,\ \varepsilon = (\pi^2 R/a^2)[D_{11}^* D_{22}^* A_{11}^* A_{22}^*]^{1/4}, \\ (W, W^*) = \varepsilon(\bar{W}, \bar{W}^*)/[D_{11}^* D_{22}^* A_{11}^* A_{22}^*]^{1/4},\ F = \varepsilon^2 \bar{F}/[D_{11}^* D_{22}^*]^{1/2}, \\ \gamma_{12} = (D_{12}^* + 2D_{66}^*)/D_{11}^*,\ \gamma_{22} = \left(A_{12}^* + \frac{1}{2}A_{66}^*\right)/A_{22}^*, \\ \gamma_{14} = [D_{22}^*/D_{11}^*]^{1/2}, \gamma_{24} = [A_{11}^*/A_{22}^*]^{1/2}, \gamma_5 = -A_{12}^*/A_{22}^*, \\ (\gamma_{30}, \gamma_{32}, \gamma_{34}, \gamma_{311}, \gamma_{322}) = (B_{21}^*, B_{11}^* + B_{22}^* - 2B_{66}^*, \\ \quad B_{12}^*, B_{11}^*, B_{22}^*)/[D_{11}^* D_{22}^* A_{11}^* A_{22}^*]^{1/4}, \\ (\gamma_{T1}, \gamma_{T2}, \gamma_{P1}, \gamma_{P2}) = (A_x^T, A_y^T, B_x^p, B_y^p) R[A_{11}^* A_{22}^*/D_{11}^* D_{22}^*]^{1/4}, \\ (M_x, M_x^p) = \varepsilon^2(\bar{M}_x, \bar{M}_x^p)(a^2/\pi^2)/D_{11}^*[D_{11}^* D_{22}^* A_{11}^* A_{22}^*]^{1/4}, \\ \lambda_p = \sigma_x/(2/Rt)[D_{11}^* D_{22}^*/A_{11}^* A_{22}^*]^{1/4}, \\ \delta_x = (\Delta_x/a)/(2/R)[D_{11}^* D_{22}^* A_{11}^* A_{22}^*]^{1/4}. \end{cases} \tag{11}$$

那么非线性方程(1)和(2)可表为如下无量纲形式

$$\varepsilon^2 L_{11}(W) + \varepsilon\gamma_{14} L_{12}(F) - \gamma_{14} F_{,xx} = \gamma_{14}\beta^2 L(W + W_T^*, F) \tag{12}$$

$$L_{21}(F) - \varepsilon\gamma_{24} L_{22}(W) + \gamma_{24} W_{,xx} = -\frac{1}{2}\gamma_{24}\beta^2 L(W + 2W_T^*, W), \tag{13}$$

其中 $W_T^* = W^* + W_{\mathrm{II}}^*$,而 W_{II}^* 为面内不可移直线边界上压应力引起的附加挠度. 对于直线边界面内可移的情况 $W_{\mathrm{II}}^* = 0$. 式(12)和(13)中所有算子如文献[5]给出.

对于大多数纤维增强复合材料 $[D_{11}^* D_{22}^* A_{11}^* A_{22}^*]^{1/4} = (0.2 \sim 0.3)t$,由式(11),当 $\bar{Z} = (a^2/Rt) > 2.96$ 时,我们有 $\varepsilon < 1$. 特别是对于各向同性圆柱曲板,我们有 $\varepsilon = \pi^2/\bar{Z}_V\beta^2[12(1$

$-\nu^2)]^{1/2}$,其中 $\bar{Z}_V(=b^2/Rt)$ 在经典的线性屈曲分析中其值应大于11.95(参见 Vol'mir[11]),在此种情况下,$\varepsilon<1$ 的条件总能满足,除非 $\beta<0.5$. 当 $\varepsilon<1$ 时,方程(12)和(13)即为边界层型方程. 此方程可以同时考虑曲板非线性前屈曲变形、后屈曲大挠度和初始几何缺陷的影响.

边界条件式(7)化为

$x=0,\pi$:

$$W=V=0, \tag{14a}$$

$$M_x=0, \tag{14b}$$

$$\frac{1}{\pi}\int_0^{\pi}\beta^2\frac{\partial^2 F}{\partial y^2}\mathrm{d}y+2\lambda_p\varepsilon=0. \tag{14c}$$

$y=0,\pi$:

$$W=0, \tag{14d}$$

$$F_{,xy}=0, \tag{14e}$$

$$M_y(\text{或 } W_{,x})=0, \tag{14f}$$

$$\int_0^{\pi}\frac{\partial^2 F}{\partial x^2}\mathrm{d}x=0\ (\text{面内可移})\ \text{或}\ V=0\ (\text{面内不可移}). \tag{14g}$$

由式(8)表征的面内边界条件化为

$$\int_0^{\pi}\int_0^{\pi}\Big[\Big(\frac{\partial^2 F}{\partial x^2}-\gamma_5\beta^2\frac{\partial^2 F}{\partial y^2}\Big)-\varepsilon\gamma_{24}\Big(\gamma_{30}\frac{\partial^2 W}{\partial x^2}+\gamma_{322}\beta^2\frac{\partial^2 W}{\partial y^2}\Big)+\gamma_{24}W-\frac{1}{2}\gamma_{24}\beta^2\Big(\frac{\partial W}{\partial y}\Big)^2-\gamma_{24}\beta^2\frac{\partial W}{\partial y}\frac{\partial W_T^*}{\partial y}+\varepsilon(\gamma_{T2}-\gamma_5\gamma_{T1})\Delta T+\varepsilon(\gamma_{p2}-\gamma_5\gamma_{p1})\Delta V\Big]\mathrm{d}y\mathrm{d}x=0. \tag{15}$$

单位端部缩短化为

$$\delta_x=-\frac{1}{2\pi^2\gamma_{24}}\varepsilon^{-1}\int_0^{\pi}\int_0^{\pi}\Big[\Big(\gamma_{24}^2\beta^2\frac{\partial^2 F}{\partial y^2}-\gamma_5\frac{\partial^2 F}{\partial x^2}\Big)-\varepsilon\gamma_{24}\Big(\gamma_{311}\frac{\partial^2 W}{\partial x^2}+\gamma_{34}\beta^2\frac{\partial^2 W}{\partial y^2}\Big)-\frac{1}{2}\gamma_{24}\Big(\frac{\partial W}{\partial x}\Big)^2-\gamma_{24}\frac{\partial W}{\partial x}\frac{\partial W_T^*}{\partial x}+\varepsilon(\gamma_{24}^2\gamma_{T1}-\gamma_5\gamma_{T2})\Delta T+\varepsilon(\gamma_{24}^2\gamma_{p1}-\gamma_5\gamma_{p2})\Delta V\Big]\mathrm{d}y\mathrm{d}x. \tag{16}$$

注意到式(12)和(13)形式上与非对称层合圆柱曲板受机械荷载的作用的情况一致. 由于 ΔT 和 ΔV 与坐标无关,热-压电耦合效应从式(12)和(13)中消失,但式(15)和(16)中仍含有 ΔT 和 ΔV.

依据式(12)~(16),采用奇异摄动方法可确定完善和非完善,含压电作动器正交铺设层合圆柱曲板在复合荷载作用下的后屈曲行为. 假定方程(12)和(13)的解为

$$\begin{cases}W=w(x,y,\varepsilon)+\tilde{W}(x,\xi,y,\varepsilon)+\hat{W}(x,\zeta,y,\varepsilon),\\ F=f(x,y,\varepsilon)+\tilde{F}(x,\xi,y,\varepsilon)+\hat{F}(x,\zeta,y,\varepsilon),\end{cases} \tag{17}$$

其中 ε 为摄动小参数(限于 $\bar{Z}>2.96$). $w(x,y,\varepsilon),f(x,y,\varepsilon)$ 称为曲板的"外解"或正则解,$\tilde{W}(x,\xi,y,\varepsilon),\tilde{F}(x,\xi,y,\varepsilon)$ 和 $\hat{W}(x,\zeta,y,\varepsilon),\hat{F}(x,\zeta,y,\varepsilon)$ 分别为 $x=0$ 和 $x=\pi$ 端的边界层解,且边界层变量 ξ 和 ζ 定义为

$$\xi=x/\sqrt{\varepsilon},\quad \zeta=(\pi-x)/\sqrt{\varepsilon} \tag{18}$$

(这意味着对于各向同性圆柱曲板,边界层宽度为 $\sqrt{Rt}$ 量级). 将式(17)中的正则解和边界层解展为如下渐近展开式

$$w(x,y,\varepsilon)=\sum_{j=1}\varepsilon^j w_j(x,y),\ f(x,y,\varepsilon)=\sum_{j=0}\varepsilon^j f_j(x,y), \tag{19a}$$

$$\tilde{W}(x,\xi,y,\varepsilon)=\sum_{j=0}\varepsilon^{j+1}\tilde{W}_{j+1}(x,\xi,y),\tilde{F}(x,\xi,y,\varepsilon)=\sum_{j=0}\varepsilon^{j+2}\tilde{F}_{j+2}(x,\xi,y), \tag{19b}$$

$$\hat{W}(x,\zeta,y,\varepsilon)=\sum_{j=0}\varepsilon^{j+1}\hat{W}_{j+1}(x,\zeta,y),\hat{F}(x,\zeta,y,\varepsilon)=\sum_{j=0}\varepsilon^{j+2}\hat{F}_{j+2}(x,\zeta,y). \tag{19c}$$

曲板初始屈曲模态假定为

$$w_2(x,y)=A_{11}^{(2)}\sin mx\sin ny, \tag{20}$$

曲板初始几何缺陷假定具有相同的形式，即

$$W^*(x,y,\varepsilon)=\varepsilon^2 a_{11}^*\sin mx\sin ny. \tag{21}$$

将式(17)～(19)代入方程(12)和(13)，可得正则解和边界层解各自应满足的三组摄动方程，利用式(20)和(21)逐级求解这些摄动方程组，并在曲板 $x=0$ 和 $x=\pi$ 两端匹配正则解和边界层解，可以导得大挠度渐近解

$$\begin{aligned}W=\varepsilon\Big[&A_{00}^{(1)}-A_{00}^{(1)}\Big(\cos\phi\frac{x}{\sqrt{\varepsilon}}-\frac{c_1}{2\alpha\phi}\sin\phi\frac{x}{\sqrt{\varepsilon}}\Big)\exp\Big(-\alpha\frac{x}{\sqrt{\varepsilon}}\Big)-\\&A_{00}^{(1)}\Big(\cos\phi\frac{\pi-x}{\sqrt{\varepsilon}}-\frac{c_1}{2\alpha\phi}\sin\phi\frac{\pi-x}{\sqrt{\varepsilon}}\Big)\exp\Big(-\alpha\frac{\pi-x}{\sqrt{\varepsilon}}\Big)\Big]+\\&\varepsilon^2[A_{11}^{(2)}\sin mx\sin ny+A_{02}^{(2)}(\cos 2ny-1)-\\&A_{02}^{(2)}(\cos 2ny-1)\Big(\cos\phi\frac{x}{\sqrt{\varepsilon}}-\frac{c_1}{2\alpha\phi}\sin\phi\frac{x}{\sqrt{\varepsilon}}\Big)\exp\Big(-\alpha\frac{x}{\sqrt{\varepsilon}}\Big)-\\&A_{02}^{(2)}(\cos 2ny-1)\Big(\cos\phi\frac{\pi-x}{\sqrt{\varepsilon}}-\frac{c_1}{2\alpha\phi}\sin\phi\frac{\pi-x}{\sqrt{\varepsilon}}\Big)\exp\Big(-\alpha\frac{\pi-x}{\sqrt{\varepsilon}}\Big)\Big]+\\&\varepsilon^3[A_{11}^{(3)}\sin mx\sin ny+A_{02}^{(3)}(\cos 2ny-1)]+\varepsilon^4[A_{00}^{(4)}+A_{20}^{(4)}\cos 2mx+\\&A_{02}^{(4)}(\cos 2ny-1)+A_{13}^{(4)}\sin mx\sin 3ny+A_{04}^{(4)}(\cos 4ny-1)]+O(\varepsilon^5),\end{aligned} \tag{22}$$

$$\begin{aligned}F=&-B_{00}^{(0)}\frac{y^2}{2}+\varepsilon\Big[-B_{00}^{(1)}\frac{y^2}{2}\Big]+\varepsilon^2\Big[-B_{00}^{(2)}\frac{y^2}{2}+B_{11}^{(2)}\sin mx\sin ny+\\&A_{00}^{(1)}\Big(b_{01}^{(2)}\cos\phi\frac{x}{\sqrt{\varepsilon}}+b_{10}^{(2)}\sin\phi\frac{x}{\sqrt{\varepsilon}}\Big)\exp\Big(-\alpha\frac{x}{\sqrt{\varepsilon}}\Big)+\\&A_{00}^{(1)}\Big(b_{01}^{(2)}\cos\phi\frac{\pi-x}{\sqrt{\varepsilon}}+b_{10}^{(2)}\sin\phi\frac{\pi-x}{\sqrt{\varepsilon}}\Big)\exp\Big(-\alpha\frac{\pi-x}{\sqrt{\varepsilon}}\Big)\Big]+\\&\varepsilon^3\Big[-B_{00}^{(3)}\frac{y^2}{2}+B_{02}^{(3)}\cos 2ny+\\&A_{02}^{(2)}(\cos 2ny-1)\Big(b_{01}^{(3)}\cos\phi\frac{x}{\sqrt{\varepsilon}}+b_{10}^{(3)}\sin\phi\frac{x}{\sqrt{\varepsilon}}\Big)\exp\Big(-\alpha\frac{x}{\sqrt{\varepsilon}}\Big)+\\&A_{00}^{(2)}(\cos 2ny-1)\Big(b_{01}^{(3)}\cos\phi\frac{\pi-x}{\sqrt{\varepsilon}}+b_{10}^{(3)}\sin\phi\frac{\pi-x}{\sqrt{\varepsilon}}\Big)\exp\Big(-\alpha\frac{\pi-x}{\sqrt{\varepsilon}}\Big)\Big]+\\&\varepsilon^4[-B_{00}^{(4)}\frac{y^2}{2}-b_{00}^{(4)}\frac{x^2}{2}+B_{11}^{(4)}\sin mx\sin ny+B_{20}^{(4)}\cos 2mx+\\&B_{02}^{(4)}\cos 2ny+B_{13}^{(4)}\sin mx\sin 3ny]+O(\varepsilon^5).\end{aligned} \tag{23}$$

需要指出，对于直线边界面内可移的情况式(23)中 $b_{00}^{(4)}=0$. 为了满足沿 $y=0,\pi$ 直线边界 $w_1=0$ 的条件，将式(22)中 $A_{00}^{(1)}$ 沿 y 向展成 Fourier 级数，即

$$\frac{4}{\pi}A_{00}^{(1)}\sum_{j=1,3,\cdots}\frac{1}{j}\sin jy, \tag{24}$$

而在 x 向仍保持为常数. 由式(22)可见,由于边界层解的贡献,曲板前屈曲变形是非线性的.

式(22)和(23)中各系数相互联系,皆可表为 $A_{11}^{(2)}$ 的函数,为简洁起见,具体表达式不再给出,但 c_1,α 和 ϕ 将在附录中给出.

进一步,将式(22)和(23)代入边界条件(14c)及式(15)和(16),我们可以导得后屈曲平衡路径

$$\lambda_p = \lambda_p^{(0)} - \lambda_p^{(2)}(A_{11}^{(2)}\varepsilon)^2 + \lambda_p^{(4)}(A_{11}^{(2)}\varepsilon)^4 + \cdots, \tag{25}$$

和

$$\delta_x = \delta_x^{(0)} - \delta_x^{(P)} + \delta_x^{(2)}(A_{11}^{(2)}\varepsilon)^2 + \delta_x^{(4)}(A_{11}^{(2)}\varepsilon)^4 + \cdots, \tag{26}$$

式(25)和(26)中,$(A_{11}^{(2)}\varepsilon^2)$ 可视为二次摄动参数,其值与曲板最大无量纲挠度有关,即

$$A_{11}^{(2)}\varepsilon = W_m - \Theta_3 W_m^2 + \cdots, \tag{27a}$$

其中 W_m 为曲板最大无量纲挠度,假定取在$(x,y) = (\pi/2m,\pi/2n)$ 点,且

$$W_m = \frac{1}{C_3}\left[\frac{t}{[D_{11}^* D_{22}^* A_{11}^* A_{22}^*]^{1/4}}\frac{\bar{W}}{t} + \Theta_4\right]. \tag{27b}$$

式(25)~(27)中所有其它符号在附录中给出.

式(25)~(27)可用于含压电作动器正交铺设层合圆柱曲板在复合荷载作用下的后屈曲荷载-端部缩短曲线和荷载-挠度曲线计算. 对于完善曲板 $\bar{W}^*/t = 0$(或 $\mu = 0$),并取 $\bar{W}/t = 0$(注意 $W_m \neq 0$),我们容易求得屈曲荷载,其相应的屈曲模态为(m,n),分别对应 X 向和 Y 向的半波数. 需要注意,对于直线边界面内不可移的情况,在后屈曲平衡路径上仅能得到极值点荷载.

3 数值算例和讨论

为了研究热-压电效应对混合层合圆柱曲板后屈曲的影响,本节给出完善和非完善,含整体覆盖或内埋压电作动器正交铺设层合圆柱曲板的数值结果. 正交各向异性层板选用石墨/环氧复合材料,材料性能参数取为: $E_{11} = 150$ GPa, $E_{22} = 9.0$ GPa, $G_{12} = 7.1$ GPa, $\nu_{12} = 0.3$, $\alpha_{11} = 1.1\times10^{-6}/(℃)$, $\alpha_{22} = 25.2\times10^{-6}/(℃)$;压电层选用压电陶瓷(PZT-5A),材料性能参数取为: $E_{11} = E_{22} = 63$ GPa, $G_{12} = 24.2$ GPa, $\nu_{12} = 0.3$, $\alpha_{11} = \alpha_{22} = 0.9\times10^{-6}/(℃)$ 和 $d_{31} = d_{32} = 2.54\times10^{-10}$ m/V. 在所有算例中(除表 1 和 2),压电层厚度为 0.1 mm,纤维增强复合材料层板总厚为 1.0 mm,且各层具有相同厚度.

表 1 (0/90/0)对称正交铺设层合圆柱曲板屈曲荷载 $N_{cr}/(E_{22}t^3)$ 比较

$(E_{11}/E_{22} = 25, G_{12}/E_{22} = G_{13}/E_{22} = 0.5, G_{23}/E_{22} = 0.2, \nu_{12} = 0.25, a/b = 1.0, b/t = 100)$

	文献[12]		本文	
a/R	CLT	FSDT	CLT	HSDT②
5	788.7(3,6)①	772.1(3,6)	788.69(3,6)	766.593(3,6)
2	324.2(2,4)	320.9(2,4)	324.23(2,4)	319.721(2,4)
1	165.2(1,2)	164.9(1,2)	165.14(1,2)	164.857(1,2)

① 括号里的值表示屈曲模态 (m,n),

② 采用文献[16]的解.

表 2　反对称正交铺设层合圆柱曲板屈曲荷载($N_{cr}/E_{22}R$) × 10^3 比较

(E_{11}/E_{22} = 40, G_{12}/E_{22} = 0.6, ν_{12} = 0.25, a/R = 1.0)

铺层	a/R	b/t	文献[13]	本文
$(0/90)_T$	1.0	100	0.182①(3,3)②	0.1805(3,3)
	1.25	80	0.176(3,2)	0.176 9(3,2)
$(0/90)_{2T}$	1.0	100	0.265(2,2)	0.265 1(2,2)
	1.25	80	0.294(3,2)	0.293 0(3,2)

① 由文献[13]曲线上读得的值

② 括号里的值表示屈曲模态 (m, n)

表 3　混合层合圆柱曲板在复合荷载作用下的屈曲荷载 P_{cr}(kN) 比较

(b/t = 200, a/b = 1.0, a/R = 0.2)

	ΔT = 0℃			
	$(P/(0/90)_2)_S$	$(0/P/90/0/90)_S$	$(P/(0/90)_4/P)_T$	$(0/P(90/0)_3/P/90)_T$
$V_U = V_L = -100$V	7.761 6(2,2)①	7.428 0(2,2)	7.687 3(2,2)	7.282 4(2,2)
$V_U = V_L = 0$V	7.760 2	7.427 2	7.686 1	7.281 9
$V_U = V_L = 100$V	7.734 6	7.401 6	7.661 2	7.257 8
	ΔT = 200℃			
	$(P/(0/90)_2)_S$	$(0/P/90/0/90)_S$	$(P/(0/90)_4/P)_T$	$(0/P(90/0)_3/P/90)_T$
$V_U = V_L = -100$V	6.707 9(2,2)①	6.408 4(2,2)	6.613 6(2,2)	6.214 7(2,2)
$V_U = V_L = 0$V	6.533 4	6.249 3	6.427 2	6.028 6
$V_U = V_L = 100$V	6.353 7	6.089 1	6.232 1	5.83 7

① 括号里的值表示屈曲模态 (m, n)

表 4　混合层合圆柱曲板在复合荷载作用下的缺陷敏感度 λ^* 比较

(b/t = 200, a/b = 1.0, a/R = 0.2)

铺层	V_U/V = V_L/V	$\bar{W}^*/t$ = 0.0	$\bar{W}^*/t$ = 0.05	$\bar{W}^*/t$ = 0.1	$\bar{W}^*/t$ = 0.15	$\bar{W}^*/t$ = 0.2	$\bar{W}^*/t$ = 0.3
$(P/(0/90)_2)_S$	-100	1.0	0.788 9	0.685 9	0.610 5	0.5512	…
	0	1.0	0.789 1	0.686 0	0.610 6	0.551 3	…
	+100	1.0	0.791 7	0.688 3	0.612 6	0.551 3	…
$(0/P/90/0/90)_S$	-100	1.0	0.784 5	0.680 5	0.605 7	…	…
	0	1.0	0.784 6	0.680 6	0.605 8	…	…
	+100	1.0	0.787 3	0.682 9	0.607 9	…	…
$(P/(0/90)_4/P)_T$	-100	1.0	0.789 9	0.686 9	0.610 8	0.550 2	0.458 5
	0	1.0	0.790 1	0.687 0	0.610 9	0.550 3	0.458 6
	+100	1.0	0.792 6	0.689 2	0.612 8	0.552 1	0.460 0
$(0/P(90/0)_3/P/90)_T$	-100	1.0	0.786 6	0.682 1	0.605 1	0.543 9	0.451 3
	0	1.0	0.786 6	0.682 2	0.605 2	0.544 0	0.451 4
	+100	1.0	0.789 2	0.684 4	0.607 2	0.545 8	0.452 9

作为部分验证，表 1 给出(0/90/0)对称层合圆柱曲板在轴压作用下的屈曲荷载并与 Carrera[12]解的比较，其中材料性能参数取为：E_{11}/E_{22} = 25, G_{12}/E_{22} = 0.5, ν_{12} = 0.25. 表 2 给出反对称正交铺设层合圆柱曲板在轴压作用下的屈曲荷载并与 Turvey[13]解的比较，其中材料性

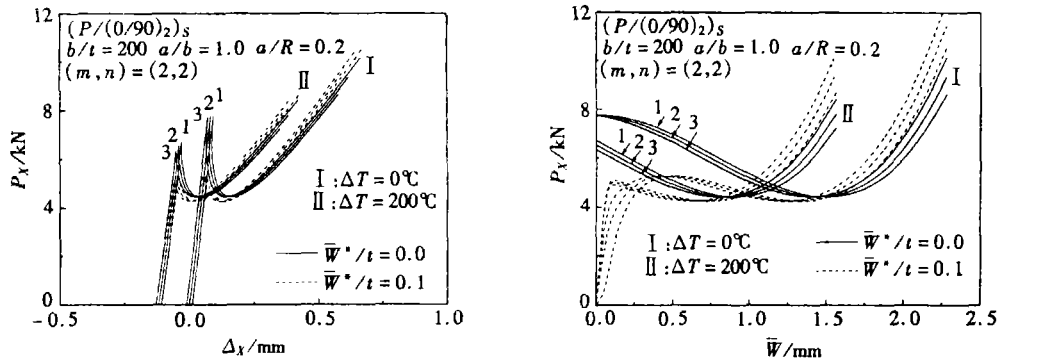

(a) 荷载-端部缩短曲线 (b) 荷载-挠度曲线

图 2 热-压电效应对 $(P/(0/90)_2)_S$ 混合层合圆柱曲板后屈曲的影响

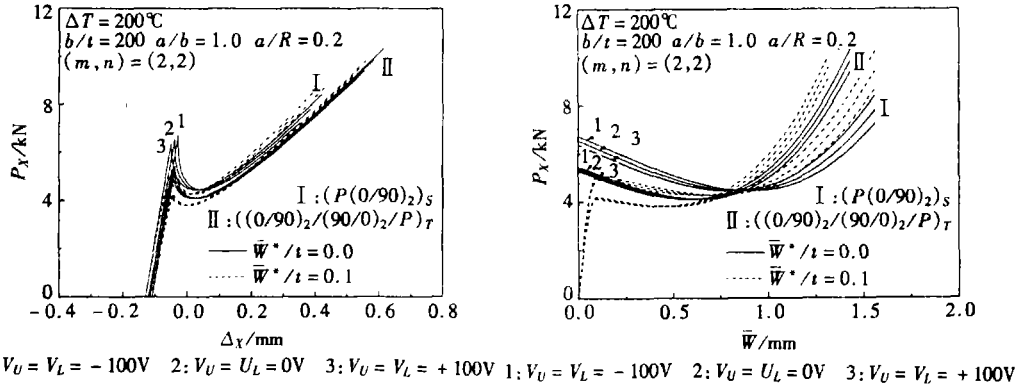

(a) 荷载-端部缩短曲线 (b) 荷载-挠度曲线

图 3 $(P/(0/90)_2)_S$ 和 $(0/90)_2/(90/0)_2/P)_T$ 混合层合圆柱曲板在复合荷载作用下后屈曲比较

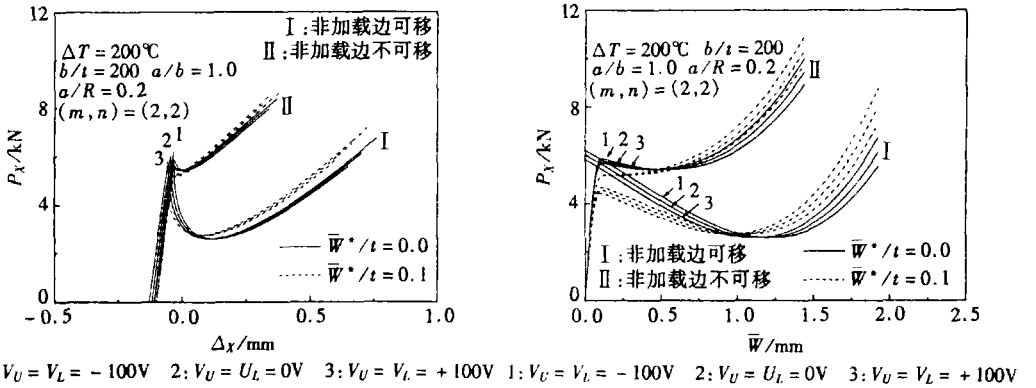

(a) 荷载-端部缩短曲线 (b) 荷载-挠度曲线

图 4 对应两种面内边界条件，$(0/P/(0/90)_3/P/90)_T$ 混合层合圆柱曲板在复合荷载作用下后屈曲比较

能材料取为：$E_{11}/E_{22}=40, G_{12}/E_{22}=0.6, \nu_{12}=0.25$. 需要指出，由于存在拉-弯耦合效应，对于反对称正交铺设层合圆柱曲板文献[14]认为不存在分支点荷载，这对平板是正确的，但对

圆柱曲板"壳型"屈曲荷载仍可求得[12,13,15],尽管前曲变形是非线性的.

表3和图2~4为参数分析的主要结果. 所有图中 $\bar{W}^*/t$ 表示曲板无量纲初始几何缺陷. 曲板几何参数取作 $a/b = 1.0, b/t = 200$ 和 $a/R = 0.2$. 直线边界为面内可移,除非有特别说明. 为简明起见, $(0/90)_{2S}$ 对称铺设和 $(0/90)_{4T}$ 反对称铺设层合圆柱曲板含对称整体覆盖或内埋压电作动器分别记作 $(P/(0/90)_2)_S$, $(0/P/90/0/90)_S$, $(P/(0/90)_4/P)_T$ 和 $(0/P/(90/0)_3/P/90)_T$,而 $(0/90)_{2S}$ 对称铺设层合圆柱曲板仅在下表面带有整体覆盖压电作动器的记为 $((0/90)_2/(90/0)_2/P)_T$.

表3给出完善混合层合圆柱曲板在复合荷载作用下的屈曲荷载比较. 热环境记作Ⅰ和Ⅱ. Ⅰ对应 $\Delta T = 0℃$, Ⅱ 对应 $\Delta T = 200℃$. 取控制电压上下相等,分别记为 V_U 和 V_L. 考虑三种外加电压状态, $V_U = V_L = -100V, 0V, +100V$. 其中 $V_U = V_L = 0V$ 对应接地状态. 计算表明,在相同温度条件下控制电压对屈曲荷载只有小的影响.

图2给出 $(P/(0/90)_2)_S$ 混合层合圆柱曲板在复合荷载作用下的后屈曲荷载-端部缩短和荷载-挠度曲线. 图示表明,控制电压对后屈曲行为也只有小的影响,并且这种影响随着挠度的增加而增加. 由图2可见壳体"跳跃"式的后屈曲平衡路径,据此可计算曲板的缺陷敏感度.

图3给出 $(P/(0/90)_2)_S$ 和 $((0/90)_2/(90/0)_2/P)_T$ 混合层合圆柱曲板在复合荷载作用下的后屈曲荷载-端部缩短和荷载-挠度曲线比较. 图示表明, $((0/90)_2/(90/0)_2/P)_T$ 圆柱曲板有较低的屈曲荷载,但在 $\bar{W}/t > 0.8$ 的范围内有较高的后屈曲荷载. 注意此时 $((0/90)_2/(90/0)_2/P)_T$ 圆柱曲板的总厚度为 $t = 1.1$ mm,并且仅有 V_L 作用.

图4给出对应两种面内边界条件时 $(0/P/(90/0)_3/P/90)_T$ 混合层合圆柱曲板在复合荷载作用下的后屈曲荷载-端部缩短和荷载-挠度曲线比较. 图示表明,非加载直线边界为面内不可移时会引起附加挠度,且仅可得到极值点荷载.

表4显示控制电压对混合层合圆柱曲板缺陷敏感度仅有很小的影响. 此处 λ^* 等于非完善圆柱曲板的极值点荷载除以完善圆柱曲板的屈曲荷载.

4 结　语

为了弄清热-压电效应对混合层合圆柱曲板后屈曲行为的影响,给出带压电作动器混合层合圆柱曲板在轴向压缩、电荷载和热荷载作用下的后屈曲分析. 假定温度场为均匀分布,电场仅有沿板厚方向的分量 E_Z,且假定材料性能常数与温度和电场的变化无关. 将壳体屈曲的边界层理论推广到混合层合圆柱曲板受复合荷载作用的情况. 相应的奇异摄动法用于确定圆柱曲板的屈曲荷载和后屈曲平衡路径. 数值算例给出完善和非完善,含整体覆盖或内埋压电作动器正交铺设层合圆柱曲板的后屈曲荷载-端部缩短和荷载-挠度曲线. 计算结果表明,在相同温度条件下控制电压对屈曲荷载和后屈曲行为只有小的影响,且各种影响随着挠度的增加而增加. 控制电压对缺陷敏感度仅有很小的影响,可以忽略. 计算结果同时表明,对于非加载直线边界面内不可移的情况后屈曲平衡路径不再是分支型的.

附　录

式(25)~(27)中

$$\Theta_3 = \frac{1}{C_3}\left\{\left(\frac{\gamma_{24}^2}{\gamma_{14}\gamma_{24} + \gamma_{34}^2}\right)\frac{m^4(1+\mu)}{8n^2\beta^2 g_2}\varepsilon^{-1} +\right.$$

$$\frac{1}{16}\left(\frac{\gamma_{24}^2}{\gamma_{14}\gamma_{24}+\gamma_{34}^2}\right)\frac{m^2}{\gamma_{24}n^2\beta^2}\left[\frac{\gamma_{34}}{\gamma_{24}}(1+2\mu)-2\gamma_{24}\frac{g_3}{g_2}\right]+\frac{2\gamma_5}{\gamma_{24}}\lambda_p^{(2)}\Big\},$$

$$\Theta_4=\frac{1}{\gamma_{24}}[(\gamma_{T2}-\gamma_5\gamma_{T1})\Delta T+(\gamma_{P2}-\gamma_5\gamma_{P1})\Delta V]+\frac{2\gamma_5}{\gamma_{24}}\lambda_p^{(2)},$$

$$\lambda_p^{(0)}=\frac{1}{2}\left\{\frac{\gamma_{24}m^2}{(1+\mu)g_2}\varepsilon^{-1}+\gamma_{24}\frac{(2+\mu)g_3}{(1+\mu)^2g_2}+\frac{1}{(1+\mu)m^2}\left[\frac{g_1}{\gamma_{14}}+\gamma_{24}\frac{g_3}{g_2}\frac{(1-\mu-\mu^2)}{(1+\mu)^2}\right]\varepsilon-\right.$$

$$\left.\frac{\mu}{(1+\mu)^2}\frac{g_3}{m^4}\left[1+\frac{g_3}{(1+\mu)m^2}\varepsilon\right]\left[\frac{g_1}{\gamma_{14}}+\gamma_{24}\frac{g_3^2}{g_2}\frac{(2+\mu)^2}{(1+\mu)^2}\right]\varepsilon^2\right\},$$

$$\lambda_p^{(2)}=\frac{1}{8}\left\{\left(\frac{\gamma_{24}^2}{\gamma_{14}\gamma_{24}+\gamma_{34}^2}\right)\frac{\gamma_{24}m^6(2+\mu)}{2g_2^2}\varepsilon^{-1}+\right.$$

$$\left(\frac{\gamma_{24}^2}{\gamma_{14}\gamma_{24}+\gamma_{34}^2}\right)\frac{m^4}{2g_2}\left[\frac{\gamma_{34}}{\gamma_{24}}\frac{(1+\mu)^2+(1+2\mu)}{1+\mu}+\mu\gamma_{24}\frac{g_3}{g_2}\right]-C_{22}+$$

$$\left(\frac{\gamma_{24}^2}{\gamma_{14}\gamma_{24}+\gamma_{34}^2}\right)\frac{m^4}{4\gamma_{24}}\left[\frac{\gamma_{34}}{\gamma_{24}}+\gamma_{24}\frac{g_3}{g_2}\frac{\mu}{1+\mu}\right]\left[\frac{\gamma_{34}}{\gamma_{24}}(1+2\mu)-2\gamma_{24}\frac{g_3}{g_2}\right]\varepsilon+$$

$$\varepsilon\frac{\gamma_{24}m^2n^4\beta^4}{g_2}\frac{g_2(5+11\mu+4\mu^2)+8m^4(1+\mu)(2+\mu)}{g_2(1+\mu)-4m^4}-$$

$$\left.\left(\frac{\gamma_{24}^2}{\gamma_{14}\gamma_{24}+\gamma_{34}^2}\right)\frac{m^2g_3}{4g_2}\left[\frac{\gamma_{34}}{\gamma_{24}}\frac{(2+5\mu+6\mu^2+2\mu^3)}{(1+\mu)^2}+2\gamma_{24}\frac{g_3}{g_2}\frac{(2+\mu)^2}{(1+\mu)^2}\right]\varepsilon\right\},$$

$$\lambda_p^{(4)}=\frac{1}{128}\left(\frac{\gamma_{24}^2}{\gamma_{14}\gamma_{24}+\gamma_{34}^2}\right)^2\frac{\gamma_{24}m^{10}(1+\mu)}{g_2^3}\frac{g_{13}(6+6\mu+\mu^2)+g_2(6-\mu^2)(1+\mu)}{g_{13}-g_2(1+\mu)}\varepsilon^{-1}+C_{44},$$

$$\delta_x^{(0)}=\frac{1}{\gamma_{24}}\left[\gamma_{24}^2-\frac{2}{\pi}\frac{\alpha}{b_1}\gamma_5^2\varepsilon^{1/2}\right]\lambda_p+\left[\frac{3\gamma_5^2}{4\pi\gamma_{24}^2}\frac{b_1}{\alpha}\varepsilon^{1/2}\right]\lambda_p^2,$$

$$\delta_x^{(2)}=\frac{1}{16}\left[d_{22}(1+2\mu)\varepsilon-2g_3\varepsilon^2+\frac{g_3^2}{m^2}\varepsilon^3\right].$$

$$\delta_x^{(4)}=\frac{1}{128}\left\{\frac{b_1}{32\pi\alpha}\left(\frac{\gamma_{24}^2}{\gamma_{14}\gamma_{24}+\gamma_{34}^2}\right)\frac{m^8(1+\mu)^2}{n^4\beta^4g_2^2}\varepsilon^{-3/2}+d_{44}+\right.$$

$$\left.m^2n^4\beta^4(1+\mu)^2\varepsilon^3\left[\frac{g^2(1+2\mu)+8m^4(1+\mu)}{g_2(1+\mu)-4m^4}\right]^2\right\},$$

$$\delta_x^{(P)}=\frac{1}{2\gamma_{24}}[(\gamma_{24}^2\gamma_{T1}-\gamma_5\gamma_{T2})\Delta T+(\gamma_{24}^2\gamma_{P1}-\gamma_5\gamma_{P2})\Delta V],$$

(A.1)

在上式中(其中 g_1,g_2,g_3 和 g_{13} 如文献[5]所给出)

$$\begin{cases}\alpha=\left[\frac{b_1-c_1}{2}\right]^{1/2},\ \phi=\left[\frac{b_1+c_1}{2}\right]^{1/2},\ b_1=\left(\frac{\gamma_{14}\gamma_{24}}{1+\gamma_{14}\gamma_{24}\gamma_{30}^2}\right)^{1/2},\\ c_1=-\frac{\gamma_{14}\gamma_{24}\gamma_{30}}{1+\gamma_{14}\gamma_{24}\gamma_{30}^2},\ C_3=1-\frac{g_3}{m^2}\varepsilon,\ \mu=(a_{11}^*+A_{\text{II}}^*)/A_{11}^{(2)}.\end{cases}\tag{A.2}$$

对于直线边界面内不可移情况

$$\begin{cases}A_{\text{II}}^*=\frac{2\gamma_{14}\gamma_{24}n^2\beta^2}{\pi^2mng_1}(1+2\mu)(A_{11}^{(2)})^2,\ C_{22}=\frac{1}{4\gamma_{24}}\frac{(m^4+2\gamma_{24}^2n^4\beta^4)}{m^2}(1+2\mu)\varepsilon,\\ C_{44}=\frac{1}{128}\left(\frac{\gamma_{24}^2}{\gamma_{14}\gamma_{24}+\gamma_{34}^2}\right)\frac{m^6(1+\mu)^2}{4g_2^2},\ d_{44}=\frac{\gamma_5}{4\gamma_{24}}\left(\frac{\gamma_{24}^2}{\gamma_{14}\gamma_{24}+\gamma_{34}^2}\right)^2\frac{m^8(1+\mu)^2}{n^2\beta^2g_2^2}\varepsilon^{-1}.\\ d_{22}=m^2+\gamma_5n^2\beta^2.\end{cases}\tag{A.3}$$

对于直线边界面内可移情况

$$A_{\text{II}}^*=0,\ C_{22}=\frac{1}{4\gamma_{24}}m^2(1+2\mu)\varepsilon,\ C_{44}=d_{44}=0,d_{22}=m^2.\tag{A.4}$$

[参 考 文 献]

[1] Saravanos D A. Mixed laminate theory and finite element for smart piezoelectric composite shell structures[J]. *AIAA Journal*, 1997, **35**(8): 1327—1333.

[2] Kapuria S, Sengupta S, Dumir P C. Three-dimensional piezothermoelastic solution for shape control of cylindrical panel[J]. *Journal of Thermal Stresses*, 1997, **20**(1): 67—85.

[3] Malik M, Noor A K. Accurate determination of transverse normal stresses in hybrid laminated panels subjected to electro-thermo-mechanical loadings[J]. *International Journal for Numerical Methods in Engineerning*, 2000, **47**(1): 477—495.

[4] Oh I K, Han J H, Lee I. Postbuckling and vibration characteristics of piezolaminated composite plate subjected to thermo-piezoelectric loads[J]. *Journal of Sound and Vibration*, 2000, **233**(1): 19—40.

[5] SHEN Hui-shen. Postbuckling of axially-loaded laminated cylindrical shells with piezoelectric actuators[J]. *European Journal of Mechanics A/Solids*, 2001, **20**(6): 1007—1022.

[6] SHEN Hui-shen. Thermal postbuckling analysis of laminated cylindrical shells with piezoelectric actuators[J]. *Composite Structures*, 2002, **55**(1): 13—22.

[7] 沈惠申, 陈铁云. 圆柱薄壳在外压作用下屈曲的边界层理论[J]. 应用数学和力学, 1988, **9**(6): 557—571.

[8] SHEN Hui-shen, CHEN Tie-yun. A boundary layer theory for the buckling of thin cylindrical shells under axial compression[A]. In: CHIEN Wei-zang, FU Zi-zhi Eds. *Advances in Applied Mathematics and Mechanics in China*[C]. Vol 2. Beijing: International Academic Publishers, 1990, 155—172.

[9] Tsai S W, Hahn H T. *Introduction to Composite Materials*[M]. Westport, CT: Technomic Publishing Co, 1980.

[10] *Guide to Modern Piezoelectric Ceramics*[M]. Bedford: Morgan Matroc Inc, 1993.

[11] Vol'mir A A. Flexible Plates and Shells[R]. AFFDL-TR-66-216, 1967.

[12] Carrera E. The effects of shear deformation and curvature on the buckling and vibrations of cross-ply laminated composite shells[J]. *Journal of Sound and Vibration*, 1991, **150**(3): 405—433.

[13] Turvey G J. Buckling of simply supported cross-ply cylindrical panels on elastic foundations[J]. *Aeronautical Journal*, 1977, **81**(794): 88—91.

[14] Zhang Y, Matthews F L. Large deflection behavior of simply supported laminatd panels under in-plane loading[J]. *Journal of Applied Mechanics ASME*, 1985, **52**: 553—558.

[15] Ye J, Soldatos K P. Three-dimensional buckling analysis of laminated composite hollow cylinders and cylindrical panels[J]. *International Journal of Solids and Structures*, 1995, **32**(13): 1949—1962.

[16] SHEN Hui-shen. Postbuckling of axially-loaded shear deformable laminated cylindrical panels[J]. *Journal of Strain Analysis for Engineering Design*, 2002, **37**(5): 413—425.

Thermo-Piezoelectric Effects on the Postbuckling of Axially-Loaded Hybrid Laminated Cylindrical Panels

SHEN Hui-shen

(*School of Civil Engineering and Mechanics, Shanghai Jiaotong University, Shanghai* 200030, *P. R. China*)

Abstract: A compressive postbuckling analysis is presented for a laminated cylinderical panel with piezoelectric actuators subjected to the combined action of mechanical, electrical and thermal loads. The temperature field considered is assumed to be a uniform distribution over the panel surface and through the panel thickness and the electric field is assumed to be the transverse component E_Z only. The material properties are assumed to be independent of the temperature and the electric field. The governing equations are based on the classical shell theory with von Kármán-Donnell-type of kinematic nonlinearity. The nonlinear prebuckling deformations and initial geometric imperfections of the panel are both taken into account. A boundary layer theory of shell buckling, which includes the effects of nonlinear prebuckling deformations, large deflections in the postbuckling range, and initial geometric imperfections of the shell, is extended to the case of hybrid laminated cylindrical panels of finite length. A singular perturbation technique is employed to determine the buckling loads and postbuckling equilibrium paths. The numerical illustrations concern the compressive postbuckling behavior of perfect and imperfect, cross-ply laminated cylindrical thin panels with fully covered or embedded piezoelectric actuators under different sets of thermal and electrical loading conditions. The effects played by temperature rise, applied voltage, stacking sequence, the character of in-plane boundary conditions, as well as initial geometric imperfections are studied.

Key words: postbuckling; hybrid laminated cylindrical panel; thermo-piezoelectric effect; boundary layer theory of shell buckling; singular perturbation technique